BEST AVAILABLE IMAGES

Defective images within this document are accurate representations of the original documents submitted by the applicant.

Defects in the images may include (but are not limited to):

- BLACK BORDERS
- TEXT CUT OFF AT TOP, BOTTOM OR SIDES
- FADED TEXT
- ILLEGIBLE TEXT
- SKEWED/SLANTED IMAGES
- COLORED PHOTOS
- BLACK OR VERY BLACK AND WHITE DARK PHOTOS
- GRAY SCALE DOCUMENTS

IMAGES ARE BEST AVAILABLE COPY.

As rescanning documents *will not* correct images, please do not report the images to the Image Problem Mailbox.

THE JOURNAL OF BIOLOGICAL CHEMISTRY
Vol. 278, No. 23, Issue of June 6, pp. 20812–20820, 2003
Printed in U.S.A.

The Methyl Donor S-Adenosylmethionine Inhibits Active Demethylation of DNA

A CANDIDATE NOVEL MECHANISM FOR THE PHARMACOLOGICAL EFFECTS OF S-ADENOSYLMETHIONINE*

Received for publication, November 20, 2002, and in revised form, March 25, 2003
Published, JBC Papers in Press, April 3, 2003, DOI 10.1074/jbc.M211813200

Nancy Detich‡§¶, Stefan Hamm§‖, George Just‡‡, J. David Knox‡, and Moshe Szyf‡§§**

*From the Departments of ‡Pharmacology and Therapeutics and **Chemistry, McGill University, Montreal, Quebec H3G 1YG, Canada*

S-Adenosylmethionine (AdoMet) is the methyl donor of numerous methylation reactions. The current model is that an increased concentration of AdoMet stimulates DNA methyltransferase reactions, triggering hypermethylation and protecting the genome against global hypomethylation, a hallmark of cancer. Using an assay of active demethylation in HEK 293 cells, we show that AdoMet inhibits active demethylation and expression of an ectopically methylated CMV-GFP (green fluorescent protein) plasmid in a dose-dependent manner. The inhibition of GFP expression is specific to methylated GFP; AdoMet does not inhibit an identical but unmethylated CMV-GFP plasmid. S-Adenosylhomocysteine (AdoHcy), the product of methyltransferase reactions utilizing AdoMet does not inhibit demethylation or expression of CMV-GFP. *In vitro*, AdoMet but not AdoHcy inhibits methylated DNA-binding protein 2/DNA demethylase as well as endogenous demethylase activity extracted from HEK 293, suggesting that AdoMet directly inhibits demethylase activity, and that the methyl residue on AdoMet is required for its interaction with demethylase. Taken together, our data support an alternative mechanism of action for AdoMet as an inhibitor of intracellular demethylase activity, which results in hypermethylation of DNA.

S-Adenosylmethionine (AdoMet)[1] is the main methyl donor in numerous methyltransferase reactions in all organisms (1). The reduced derivative of 5,10-methylenetetrahydrofolate, 5-methyltetrahydrofolate, provides the methyl group for methionine and AdoMet synthesis (2). A series of rodent experiments as well as epidemiological data have suggested a correlation between diets deficient in folate or in sources of methyl groups (*i.e.* foods containing methionine, one-carbon compounds, and choline) and the risk for colorectal adenomas and cancer (3). Such diets, referred to collectively as methyl-deficient, have been shown to promote liver cancer in rodents (4, 5), and AdoMet treatment was shown to prevent the development of liver cancer in rat (6).

In light of the clinical and epidemiological data suggesting a link between AdoMet levels and cancer, it is important to understand the tumor protective mechanism of action of AdoMet, as well as the tumor promoting action of methyl-deficient diets. This is of importance not only for realizing the therapeutic potential of AdoMet, but also for unraveling basic mechanisms of tumorigenesis, especially the role of methyl group metabolism. AdoMet is the cofactor for transmethylation reactions including DNA methylation (7, 8), whereas S-adenosylhomocysteine (AdoHcy) is the product of transmethylation reactions and an inhibitor of DNMTs (9). A current model is that exogenous administration of AdoMet increases the intracellular ratio of AdoMet to AdoHcy, thus stimulating DNMT activity resulting in increased DNA methylation (6, 10). An increase in AdoHcy concentrations, even without a concomitant reduction in AdoMet results in inhibition of DNMT and DNA hypomethylation (11). Methyl-deficient diets decrease intracellular AdoMet concentration, increase AdoHcy concentrations, and trigger DNA hypomethylation (5, 12, 13). A genetic link was established between polymorphisms in the *methylenetetrahydrofolate reductase* gene encoding the enzyme catalyzing the synthesis of 5-methyltetrahydrofolate, and DNA hypomethylation (14, 15). Global hypomethylation of DNA is a hallmark of cancer (16, 17). If the mechanism of action of methyl-rich diets in cancer chemoprevention and methyl-deficient diets in cancer promotion is through changing genomic methylation status, then it implies that global hypomethylation plays a causal role in cancer. This hypothesis is supported by the observation that 5-azacytidine, a DNMT inhibitor (18) can reverse AdoMet-mediated chemoprevention of liver carcinogenesis (19).

Although it has been controversial, there is now little doubt (1) that exogenous AdoMet increases the intracellular AdoMet levels. AdoMet uptake into cells has also been verified through a high performance liquid chromatography analysis (20). A number of data support the notion that exogenous AdoMet causes hypermethylation of DNA (10, 21).

Whereas this model provides an attractively simple explanation as to the possible relationship between exogenous AdoMet administration and DNA methylation, there are a number of unresolved issues. First, increased AdoMet should increase DNMT activity only if the normal intracellular concentration of

* This work was supported in part by the National Cancer Institute of Canada and Natural Science and Engineering Research Council Canada. The costs of publication of this article were defrayed in part by the payment of page charges. This article must therefore be hereby marked "*advertisement*" in accordance with 18 U.S.C. Section 1734 solely to indicate this fact.

§ Both authors contributed equally to the results of this work.
¶ Recipient of the Canadian Institute of Health Research Doctoral Fellowship and the McGill Faculty of Medicine Internal Fellowship.
‖ Supported by postdoctoral research stipend from Deutsche Forschungsgemeinschaft.
‡‡ Supported by Grant 228183 from the Natural Science and Engineering Research Council.
§§ To whom correspondence should be addressed: 3655 Sir William Osler Promenade, Montreal, Quebec H3G 1Y6, Canada. Tel.: 514-398-7107; Fax: 514-398-6690; E-mail: mszyf@pharma.mcgill.ca.

[1] The abbreviations used are: AdoMet, S-adenosylmethionine; AdoHcy, S-adenosylhomocysteine; MBD2, methylated DNA-binding protein 2; dMTase, DNA demethylase; TSA, trichostatin A; DNMT, DNA methyltransferase; GFP, green fluorescent protein.

AdoMet is below the K_m for the enzyme, this has not been demonstrated as of yet. It is, however, possible that the main mechanism by which elevating AdoMet levels increases DNMT activity is by competing with AdoHcy, an inhibitor of DNMT. Such an indirect mechanism of activation might be relevant even if the basal level of AdoMet is above the K_m. Second, even if exogenous administration of AdoMet increases the activity of DNMT, it is not clear whether the normal level of enzyme is limiting, or whether the specificity of DNA methylation patterns is determined by the molecular activity of DNMT. There is no evidence to suggest that specific sites remain unmethylated in vertebrate genomes simply for the reason that the molecular activity of DNMT is limiting. Third, methyl-deficient diets cause hypomethylation in the liver whose cells are mostly postmitotic and do not replicate (5). If the mechanism of this hypomethylation involves only inhibition of DNMT, it could take effect only in cells that actively synthesize DNA. Because measurable demethylation is seen with these diets, this could only occur if a significant fraction of liver cells proliferate during the treatment. Whereas an increase in proliferation in the liver is seen as a consequence of methyl-deficient diets, it is not clear whether proliferation precedes or follows global hypomethylation.

The current hypothesis on the mechanism of action of AdoMet is based on the assumption that DNA methylation is a unidirectional and irreversible reaction, which is catalyzed by DNMT exclusively. However, an increasing list of data supports the hypothesis that DNA methylation *in vivo* is also fashioned by demethylase activity (22). A DNA demethylase activity was partially purified from human lung carcinoma A549 cells (23) and the protein MBD2b was shown to bear demethylase activity (24). The demethylase activity of MBD2 was disputed by several groups (25, 26), but our recent data demonstrated that ectopic MBD2/dMTase causes DNA demethylation in a promoter-specific manner (27). We therefore proposed that DNA methylation is a reversible reaction, and that the steady state DNA methylation status of a gene reflects a balance of methylation and demethylation (28, 29). Thus, it is possible that AdoMet increases methylation by inhibiting demethylation.

It is impossible to determine whether hypermethylation of a gene *in vivo* following chronic drug treatment is caused by either an increase in DNMT activity, as proposed by the current model, or inhibition of demethylase. A model system is required to study either methylation or demethylation in isolation from the reverse activity. We have recently described such a model (Fig. 1). When an unmethylated CMV-GFP plasmid is transiently transfected into the human embryonal kidney cell line HEK 293, it remains unmethylated throughout the transient transfection period up to 96 h, demonstrating that DNMTs do not target extrachromosomal DNA under the conditions of our experiment (30). When an *in vitro* methylated CMV-GFP plasmid is transiently transfected into these cells, it generally remains methylated. However, when histone acetylation is induced by trichostatin A (TSA), the plasmid is fully and actively demethylated by an endogenous demethylase activity. Because the plasmid does not replicate during the time frame of the experiment, this assay measures only active demethylation (30). This system thus allows us to determine the impact that different factors might have on demethylase activity. We have recently used this assay to illustrate that a protein that inhibits histone acetylation inhibits active demethylation in living cells (31).

In this paper we took advantage of this assay to test the hypothesis that exogenous administration of AdoMet inhibits demethylase activity in living cells. Using an *in vitro* demethylase assay, we then tested whether AdoMet inhibits both recombinant MBD2/dMTase activity extracted from infected Sf9 insect cells, as well as endogenous demethylase activity from HEK 293 cells. Taken together, our results support a new alternative hypothesis for the mechanism of action of AdoMet as a DNA hypermethylating agent.

MATERIALS AND METHODS

In Vitro Methylation of Substrates

CMV-GFP (pEGFP-C1 from Clontech; GenBank™ accession number U55763) was methylated *in vitro* by incubating 10 μg of plasmid DNA with 12 units of *Sss*I CpG methyltransferase (New England Biolabs) in the recommended buffer containing 800 μM AdoMet for 3 h at 37 °C. Twelve units of *Sss*I and 0.16 μmol of AdoMet were then added and the reaction was further incubated for 3 additional hours. The methylated plasmid was recovered by phenol/chloroform extraction and ethanol precipitation, and complete methylation was confirmed by observing full protection from *Hpa*II digestion.

Cell Culture and Transient Transfections

Human embryonal kidney HEK 293 cells (ATCC CRL 1573) were plated at a density of 7.5×10^4/well in a 6-well dish and transiently transfected with 80 ng of CMV-GFP (methylated or mock methylated) using the calcium phosphate precipitation method as described previously (32). 0.3 μM TSA was added 24 h post-transfection. After an additional 24 h, cells were treated with or without various concentrations of AdoMet or AdoHcy (2–8 mM). Cells were harvested 72 h post-transfection. Each experiment was performed in triplicate, and experiments were performed several times using different cultures of HEK 293 cells.

Western Blot Analysis

Whole cell extracts were prepared using radioimmunoprecipitation assay buffer according to the Santa Cruz Biotechnology protocol, and protein concentrations were determined using the Bradford reagent (Bio-Rad). 2.5 μg of protein were resolved on a 12.5% SDS-polyacrylamide gel and then transferred to polyvinylidene difluoride membrane (Amersham Biosciences). After blocking the nonspecific binding with 5% skim milk, GFP protein was detected using rabbit polyclonal IgG (Santa Cruz, sc-8334) at 1:500 dilution, followed by peroxidase-conjugated anti-rabbit IgG (Sigma) at 1:5000, and enhanced chemiluminescence detection kit (Amersham Biosciences). Membranes were stained with 0.2% Ponceau S (Sigma) to determine loading of total protein in each lane. Both the Western blots and Ponceau-stained membranes were quantified using NIH Image 1.62 software, and the GFP signal was normalized to the total protein (which varied only slightly) in each lane.

Southern Blot Analysis

DNA was extracted from HEK 293 cells using the DNeasy Tissue Kit (Qiagen). DNA was first digested with 50 units of *Eco*RI, followed by digestion with 20 units of either *Hpa*II or *Msp*I restriction enzymes. Samples were subjected to electrophoresis on a 1.5% agarose gel and then transferred to Hybond-N^+ membrane (Amersham Biosciences). Blots were probed with a ^{32}P-labeled CMV-GFP cDNA probe (*Ava*II-*Cfr*101 fragment) synthesized using a random priming labeling kit (Roche Diagnostics). Membranes were hybridized at 68 °C for 4–6 h in a buffer containing 0.5 M sodium phosphate, pH 6.8, 1 mM EDTA, 7% SDS, and 0.2 mg/ml herring sperm DNA. Following hybridization, the membranes were washed twice for 10 min in a 5% SDS, 0.04 M sodium phosphate, pH 6.8, 1 mM EDTA solution, and then four times for 10 min in the same solution containing 1% SDS. The demethylation assay measures the fraction of GFP molecules that were demethylated using *Hpa*II restriction enzyme, which cleaves unmethylated CCGG but does not cleave methylated CCGG sequences. The methylated GFP DNA remains intact following *Hpa*II digestion and is identical to the fragment obtained following *Eco*RI digestion (indicated by *M* in Fig. 2*B*), whereas the unmethylated GFP DNA is cleaved by *Hpa*II resulting in a 0.5-kb fragment (indicated by *U* in Fig. 2*B*). We scanned each *Hpa*II digested lane and measured the intensity of the total signal hybridizing with the GFP probe in the same *Hpa*II lane (including the unmethylated *U* and methylated *M* fragments), this value is equal to 100% of GFP molecules in the lane. We then determined the intensity of the unmethylated signal per *Hpa*II lane, and divided this value (*U*) by the total signal for GFP (U + M) in the same *Hpa*II lane. To exclude the

possibility that the *Hpa*II digestion was skewed by differences in loading, we used the ethidium bromide-stained gels as loading controls for the corresponding Southern blots. We normalized the values obtained upon the calculation [M/(U + M)] × 100 to the amount of DNA in each *Hpa*II lane as determined by quantification of the ethidium bromide-stained gels by NIH Image 1.62. The results of three independent experiments were quantified by densitometry (NIH Image 1.62).

AdoMet Preparations for in Vitro Studies

AdoMet was prepared as a 50 mM solution in distilled water by dissolving lyophilized powder (Sigma) in distilled water. AdoHcy was purchased from Sigma and dissolved in distilled water at a 50 mM concentration.

Purification of Recombinant MBD2/dMTase from Sf9 Cells

A fragment containing human MBD2/dMTase was excised from pCR2.1-dMTase (24) with *Bam*HI and *Xho*I and transferred to the Baculovirus expression transfer vector pBlueBacHis2 C (Invitrogen). PBlueBacHis2 C-MBD2/dMTase and Bac-N-Blue viral DNA were co-transfected into the Sf9 insect cell line, and recombinant viruses were isolated, identified, and amplified according to the manufacturer's protocol (Invitrogen) with no modifications. High titer P3 viral stocks were used for infections. Insect Sf9 cells were cultured in spinner flasks to a density of 2.5×10^6 cells/ml in Grace's insect cell culture medium supplemented (1×) from Invitrogen. For infection, 5×10^6 cells were plated in 10-cm tissue culture plates (Sarstedt) and allowed to settle and attach for 30 min. The culture medium was removed and was replaced with 10 ml of the same medium containing MBD2/dMTase virus at a multiplicity of infection of 10. The cells were cultured with the virus for 5 days at 27 °C and were then harvested by scraping in cold phosphate-buffered saline. Cell pellets from 10 plates were frozen and kept at −70 °C until they were used for enzyme purification. Frozen pellets were thawed in 5 ml of lysis buffer (10 mM Tris-HCl, pH 8.0, 5 mM $MgCl_2$, 500 mM NaCl, 0.05% Tween 20, 10% glycerol, and 10 mM imidazole) containing 1 μg/ml of the following protease inhibitors: aprotinin, leupeptin, and Pefablock. Protease inhibitors were added to all the solutions used in the purification. The homogenates were subjected to two cycles of freezing and thawing (5 min per step). DNA in the homogenate was sheered by passing through an 18.5-gauge needle 10 times. The extracts were then subjected to 15 cycles of sonication (10 s burst, 10 s gap per cycle at 20% of maximal output). The extracts were centrifuged at 10,000 × *g* for 35 min. The supernatant was transferred into a fresh tube and was recentrifuged for additional an 25 min at 15,000 × *g*. The extract was filtered through a 5-micron filter to remove any particulate matter and the buffer was exchanged on a PD-10 buffer exchange column (Amersham Biosciences) with buffer L (10 mM Tris-HCl, pH 8.0, 10 mM $MgCl_2$) containing 50 mM NaCl. Recombinant MBD2/dMTase was partially purified by Q-Sepharose (Amersham Biosciences) ion exchange chromatography. Q-Sepharose beads (1 ml of swollen beads) were washed extensively and pre-equilibrated with buffer L containing 50 mM NaCl and divided into 3 equal aliquots. The cell extracts were sequentially bound three times to the 3 aliquots of Q-Sepharose beads in batch in 15-ml tubes by shaking gently on a Nutator for 45 min at 4 °C. Following each binding step, the bound beads and unbound supernatant were separated by centrifugation for 2 min at 1000 × *g* and the supernatant was transferred into a new tube and bound with new pre-equilibrated beads. The bound beads from the three binding steps were joined and resuspended in lysis buffer. The beads were washed in batchs 4 times with 5 ml of buffer L + 50 mM NaCl. For each washing step, the beads were incubated with the wash solution for 15 min and then separated from the wash supernatant by centrifugation for 2 min at 1000 × *g*. Following washing, the proteins were eluted in batchs (30 min per step) with a stepwise NaCl gradient in buffer L. Each elution step was analyzed for *in vitro* demethylase activity and for the presence of the recombinant His-tagged MBD2/dMTase by a Western blot analysis using the anti-Xpress antibody from Invitrogen as previously described. MBD2/dMTase peak elution is at the 0.4 M NaCl step. No demethylase activity was observed in the same fractions prepared in a similar manner from uninfected Sf9 cells. For concentration of the 0.4 M NaCl fraction, a Microcon YM-10 concentrator (Millipore) was used at 3300 × *g* and 4 °C. Spinning time varied according to the volume, and was 25 min for 500 μl.

Extraction of Endogenous Demethylase Activity from HEK 293 Cells

10 × 10-cm tissue culture plates of HEK 293 cells were used to prepare cell extracts as outlined in the previous section. Q-Sepharose fractionation was performed also as described above and as previously described (27).

Preparation of Substrate DNA for in Vitro Demethylation Assay

Methylation of Substrate—Typically, 25 μg of DNA from *Micrococcus lysodeikticus* (Sigma, Type XI, highly polymerized) were methylated with M.*Sss*I (60 units, New England Biolabs) and AdoMet (3.2 mM, New England Biolabs) in methylation buffer (NEbuffer2, New England Biolabs) in the presence of 50 mM EDTA for 3-4 h at 37 °C. Fresh AdoMet (3.2 mM) and enzyme (40 units) were then added before incubating at 37 °C for an additional 3–4 h. To achieve complete methylation, methylation was repeated after AdoHcy, which is a product of the methylation reaction and inhibits DNA methylation, and was removed using a Microcon 10 concentrator (Millipore) according to the manufacturer's protocol. The degree of methylation was verified by methylation sensitive restriction enzyme analysis (*Msp*I-*Hpa*II digestion) on aliquots of the reaction mixture. The DNA was purified by phenol-chloroform extraction (one part of either phenol or chloroform per three parts reaction mixture). Unincorporated nucleotides were removed by a Nap5 gel filtration chromatography (Amersham Biosciences) column. The Nap5 column was equilibrated with demethylation buffer (10 mM Tris-HCl, 5 mM $MgCl_2$, pH 7.0). DNA containing fractions were combined, concentrated on a Microcon 10, and subjected to a second Nap5 desalting column. DNA containing fractions were again concentrated as described above.

[α-^{32}P]dGTP Labeling of DNA—We then prepared either methylated or unmethylated DNA that is ^{32}P-labeled at G, the 3′ neighbor of the methylated C, as previously described (33) with the following modifications. 5 μg of either methylated or unmethylated DNA in 35 μl of double distilled water were denatured and annealed to a hexanucleotide primer by boiling for 10 min in the presence of 3 μl of random hexanucleotide mixture ($0.2 A_{260}$) (Roche Diagnostics). The primed DNA was then subjected to template-directed extension with the Klenow fragment of DNA polymerase I in the presence of labeled [α-^{32}P]dGTP, either methyl-dCTP (for methylated DNA) or dCTP for unmethylated DNA, dTTP, and dATP. The 3′ phosphate of all the 5′ neighbors of G including either C or methyl-C is labeled by this procedure. The labeling was performed in polymerase buffer (50 mM NaCl, 6.6 mM Tris-HCl, 6.6 mM $MgCl_2$, 1 mM dithiothreitol, pH 7.4) with Klenow fragment I (10 units, Roche Diagnostics), methyl-dCTP (1 mM), and dCTP (1 mM), respectively, dATP, dTTP (1 mM each), and [α-^{32}P]dGTP (50 μCi, PerkinElmer Life Sciences) for 3 h at 37 °C. The reaction mixture was extracted with phenol and chloroform (one part of each per three parts reaction mixture). Trichloroacetic acid precipitation (2 ml of 10% trichloroacetic acid, 20 μg of herring sperm DNA) of an aliquot showed typically 80–95% labeling efficiency (260,000–320,000 cpm/μl, total of 150 μl). The DNA was purified by eluting it twice from a Nap5 column and concentrating on a Microcon 10 as described above with the following variation: distilled water was used for prewashing and elution in the second column. The final concentration was 5 ng/μl and the specific activity was typically $8.0–8.8 \times 10^6$ cpm/μg.

In Vitro Demethylation Assay

A typical reaction mixture (50 μl) consisted of 25 ng of ^{32}P-prelabeled DNA (prepared as described above) incubated in demethylation buffer (10 mM Tris-HCl, 5 mM $MgCl_2$, pH 7.0) with either the purified MBD2/dMTase (5 μl, ~5 ng) or the purified demethylase activity from HEK 293 cells (5 μl) for 24 h at 37 °C in either the absence or presence of AdoMet and AdoHcy, respectively. The DNA was extracted from the enzyme by incubation in 2 volumes of DNA extraction buffer (10 mM Tris-HCl, 0.5 M NaCl, 1% SDS) containing 0.1 unit of proteinase K (Roche Diagnostics) at 50 °C for 2 h. Subsequent phenol-chloroform extraction (one part of either phenol or chloroform per three parts of reaction volume) in the presence of tRNA (50 μg) as a carrier and ethanol precipitation with salt and 95% ethanol resulted in almost quantitative recovery of the input DNA. The DNA pellets were resuspended in distilled water (8 μl) and digested with micrococcal nuclease to ^{32}P-labeled 3′ mononucleotides as described elsewhere (27, 33). The labeled mononucleotides were separated by thin layer chromatography and visualized by autoradiography on a phosphorimaging plate, and the levels of cytosine (C) and 5-methylcytosine (mC) were quantified by the MCID-M4 software (Imaging Research Inc.). The percent demethylation (C/(C + mC)) was calculated per each sample and then normalized to the value obtained for the demethylase reaction in the absence of inhibitor (0 mM AdoMet/AdoHcy).

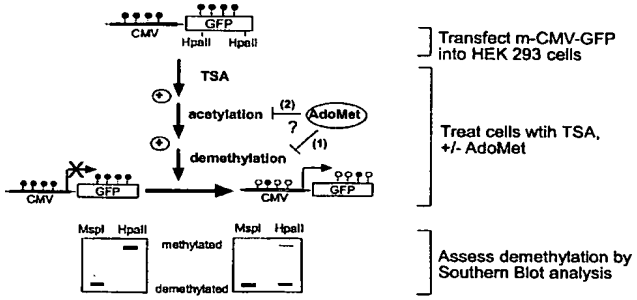

FIG. 1. **Outline of the model system used to assess the effects of AdoMet on active demethylation in living cells.** CMV-GFP plasmid is methylated *in vitro* and transiently transfected into HEK 293 cells. Histone acetylation is induced with TSA, which results in DNA demethylation by endogenous demethylase activity (30). The degree of demethylation is then measured by methylation-sensitive restriction digestion using *Hpa*II enzyme, which is followed by Southern blot analysis using a GFP-specific probe (*Ava*II-*Cfr*101 fragment). The possible mechanisms of action of AdoMet are indicated, either a direct inhibition of demethylase activity (1), or an indirect mechanism by first stimulating histone methylation and inhibiting histone acetylation, which would then inhibit active demethylation (2).

RESULTS

AdoMet Inhibits TSA-induced Active Demethylation of Ectopically Methylated and Transiently Transfected CMV-GFP in a Dose-dependent Manner—There have been several reports demonstrating that exogenous administration of AdoMet leads to DNA hypermethylation (19, 21, 35). Similarly, other studies have shown that a decrease in dietary folate, or a depletion of intracellular AdoMet, results in DNA hypomethylation (6, 12, 36, 37). However, it is not known whether the effects of AdoMet on methylation are because of changes in DNMT or DNA demethylase activities.

We utilized a previously described transient transfection-based assay system (Fig. 1 and Ref. 30) to study the effects of AdoMet on active demethylation of ectopically methylated DNA. In prior studies we have shown that the *in vitro* methylated CMV-GFP reporter plasmid is actively demethylated 72 h following transfection into HEK 293 cells when histone hyperacetylation is induced with TSA (30). Because CMV-GFP does not replicate nor is it *de novo* methylated in HEK 293 cells (30), this assay specifically measures active demethylation in a living cell.

We first determined the effects of increasing doses of AdoMet, or the product of AdoMet-dependent methyltransferase reactions, AdoHcy, on the demethylation of methylated CMV-GFP (Fig. 2). DNA was isolated from HEK 293 cells transfected with methylated CMV-GFP DNA and treated with either TSA and AdoMet, or TSA and AdoHcy. DNA was first linearized with the *Eco*RI restriction enzyme, followed by digestion with *Msp*I (which cleaves the sequence CCGG) or *Hpa*II (which cleaves the sequence CCGG only when it is not methylated). The demethylated *Hpa*II-digested 529-bp fragment (U) and the methylated *Hpa*II-undigested DNA (M) were quantified within the same lanes, and the percent methylation for CMV-GFP DNA in each lane was determined as [M/(U + M)] × 100. Values were then normalized to the total DNA per lane as determined by ethidium bromide staining. As can be seen in Fig. 2, *A* and *C*, the addition of TSA results in nearly complete demethylation of CMV-GFP by endogenous demethylase activity, as indicated by the complete *Hpa*II digestion of CMV-GFP to the 529-bp fragment (U). Upon the addition of increasing concentrations of AdoMet (Fig. 2, *B* and *D*), the percentage of methylated GFP remaining increases in a dose-dependent manner, illustrated by the decrease in the ratio of the 529-bp *Hpa*II fragment (U) to the undigested DNA (M). AdoHcy has an insignificant effect on the demethylation of CMV-GFP (Fig. 2, *B* and *D*), indicating that the methyl moiety of AdoMet is required for inhibition of demethylation.

We then determined whether AdoMet stimulates *de novo* methylation of an identical unmethylated CMV-GFP substrate. Fig. 2*E* illustrates that unmethylated CMV-GFP, transfected under identical conditions, does not get *de novo* methylated, even in the presence of 8 mM AdoMet. This indicates that AdoMet does not cause an increase in DNMT activity on ectopic CMV-GFP. Thus, the likely mechanism by which AdoMet causes hypermethylation of CMV-GFP in comparison with the TSA-treated control is by inhibiting its active demethylation by resident demethylases.

AdoMet Reduces TSA-induced Expression of Methylated CMV-GFP in a Dose-dependent Manner, but Has No Effect on Unmethylated CMV-GFP—A number of studies have shown that an increase in AdoMet inhibits gene expression (20, 21), however, it is not clear whether AdoMet specifically affects genes whose methylation state it alters exclusively, or whether it has a nonspecific effect on gene expression. We took advantage of the CMV-GFP system described above to address this question. We determined whether AdoMet influences the expression of either methylated CMV-GFP, whose methylation state is affected by AdoMet, or unmethylated CMV-GFP, whose methylation state is not affected by AdoMet. HEK 293 cells were transiently transfected and treated with TSA and either AdoMet or AdoHcy, as described in the previous section. Extracts were then prepared and subjected to a Western blot analysis using an antibody directed against GFP protein.

Fig. 3, *A* and *C*, illustrates that methylated CMV-GFP is completely repressed in untreated HEK 293 cells. This is as expected, because it is well documented that DNA methylation leads to gene silencing. The addition of TSA leads to a dramatic induction of GFP expression as expected from the complete demethylation following TSA treatment. Upon the addition of increasing amounts of AdoMet, GFP expression is decreased in a dose-dependent fashion. AdoHcy has no significant effect on the expression of methylated GFP, consistent with its lack of effect of DNA demethylation.

Because our system measures expression and demethylation that is dependent on histone hyperacetylation, there are two possible mechanisms whereby AdoMet exerts its effects on demethylation (Fig. 1). AdoMet could directly inhibit a demethylase activity, or it could inhibit histone acetylation, which we have previously shown leads to an inhibition of demethylation (30). If the latter were true, then AdoMet should also inhibit the TSA-induced expression of unmethylated GFP, whose expression is induced by histone acetylation as well. Fig. 3, *B* and *D*, indicates that this is not the case, because AdoMet has no significant effect on the induction of unmethylated GFP by TSA. The fact that AdoMet specifically affects the expression of a methylated copy of CMV-GFP, and not an unmethylated copy, supports the model that AdoMet inhibits gene expression by directly inhibiting the active demethylation of methylated CMV-GFP.

AdoMet but Not AdoHcy Inhibits Demethylation Activity in Vitro—To further confirm that the observed effect of AdoMet and AdoHcy is because of inhibition of active demethylation and not an indirect effect, *in vitro* studies with a recombinant MBD2/dMTase (the only demethylase characterized thus far) were performed (24). Because it is not certain whether MBD2/dMTase is responsible for the demethylation seen in HEK 293 cells, we also performed these studies with purified endogenous demethylase activity from HEK 293 cells. Together, these *in*

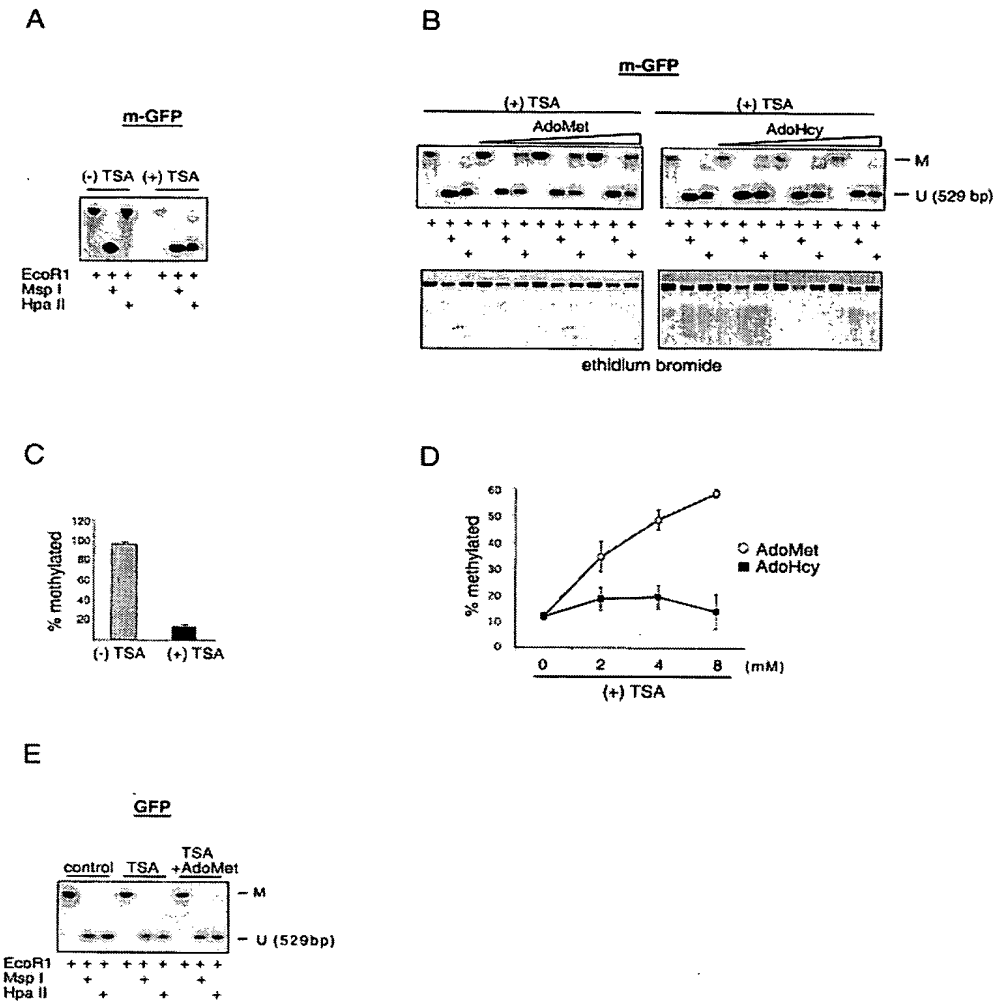

FIG. 2. **AdoMet inhibits active demethylation of CMV-GFP.** *A*, *B*, and *E*, either *in vitro* methylated CMV-GFP plasmid (*m-GFP*) (*A* and *B*), or unmethylated CMV-GFP (GFP) (*E*) were transiently transfected into HEK 293 cells. Cells were treated with a final concentration of 0.3 μM TSA (+*TSA*), or left untreated (−*TSA*), and increasing concentrations of either AdoMet or AdoHcy (2, 4, and 8 mM) were added. Cells were harvested 72 h post-transfection, and the methylation status of CMV-GFP was determined by *MspI*/*Hpa*II restriction digestion and Southern blot analysis as outlined under "Materials and Methods" and in the legend to Fig. 1. *M*, methylated and *Hpa*II undigested GFP; *U*, unmethylated and *Hpa*II fully digested GFP (529 bp); *B*, *lower panel*, ethidium bromide-stained gels. *C*, the results of three independent experiments as shown in *A* were quantified by densitometry, and the average percent methylation remaining for each sample was calculated as outlined under "Materials and Methods" and charted ± S.D. *D*, the results of three independent experiments as shown in *B* were quantified as in *C* and the averages ± S.D. are presented. ○, AdoMet; □, AdoHcy.

vitro experiments should test whether AdoMet can act as an inhibitor of one or more demethylase activities.

First, His-tagged MBD2/dMTase was partially purified by chromatography on Q-Sepharose from cell extracts of Sf9 cells infected with the recombinant MBD2/dMTase construct as described under "Materials and Methods." Fractions were eluted with a stepwise gradient of NaCl and assayed for demethylation activity with a ^{32}P-prelabeled methylated DNA from *M. lysodeikticus* (Fig. 4, *A*, *left panel*). Conversion of methyl-dCMP to dCMP, whereas not extensive, was almost exclusively detected with the 0.4 M NaCl fraction (16% demethylation). This correlates with the peak presence of the His-tagged recombinant MBD2/dMTase protein in this fraction as demonstrated by Western blot analysis (Fig. 4*B*) using an anti-Xpress antibody. To confirm that the 0.4 M NaCl fraction contained demethylase activity, the fraction was concentrated 10-fold on a Microcon concentrator. As expected, the demethylase activity in the 0.4 M NaCl fraction increased accordingly (Fig. 4*A*, *right panel*); 5 μl of the concentrated fraction completely converted methyl-dCMP to dCMP for the same amount of DNA as used before (Fig. 4*A*, *left panel*).

Next, we determined whether AdoMet inhibits the demethylation activity of MBD2/dMTase. The aforementioned DNA was incubated with MBD2/dMTase from Sf9 cells in the presence of increasing AdoMet concentrations, and conversion of methyl-dCMP (mC) to dCMP (C) was assessed as above. Fig. 5*A* presents the autoradiography and quantification of one representative experiment. Because of the numerous steps involved in this assay, it is impossible to avoid small loading differences between samples. To determine percent activity, the percent demethylation, (C/(C + mC)), was thus calculated within each sample to control for these differences, and then normalized to

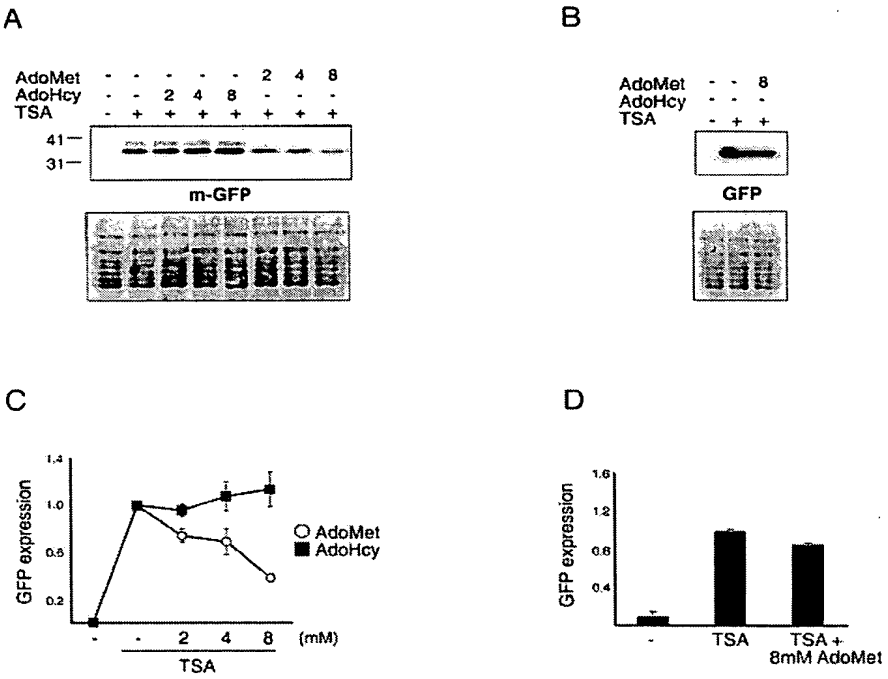

FIG. 3. **AdoMet reduces TSA-induced expression of methylated CMV-GFP.** *A* and *B*, HEK 293 cells were transiently transfected with either methylated CMV-GFP plasmid (m-GFP) (*A*) or unmethylated CMV-GFP (*GFP*) (*B*) and treated with 0.3 μM TSA and with the indicated concentrations (mM) of AdoMet or AdoHcy. Total cell extracts were prepared using standard protocols and resolved on a 12.5% SDS-polyacrylamide gel. Proteins were transferred to polyvinylidene difluoride membrane, and GFP protein was detected using rabbit polyclonal IgG (Santa Cruz, sc-8334). Membranes were stained with Ponceau S to show equal loading. *C*, experiments such as those shown in *A* were performed in triplicate and quantified by densitometry. Results are presented as arbitrary units relative to the level of GFP expression in the presence of TSA alone that was normalized to one. ○, AdoMet; □, AdoHcy. *D*, quantification of triplicate experiments as shown in *B*; the averages ± S.D. are presented.

the value obtained for the demethylase reaction in the absence of inhibitor (0 mM AdoMet/AdoHcy). Conversion of methyl-dCMP to CMP was greatly reduced at 0.5 mM AdoMet and abolished completely at concentrations higher than 0.7 mM.

In contrast to AdoMet, no inhibition of demethylation occurred in the presence of increasing concentrations of AdoHcy (Fig. 5*B*). These results indicate that the small differences in the chemical structure (methyl group and positive charge on the sulfur) between AdoMet and AdoHcy are responsible for their different interactions with the MBD2/dMTase.

To test whether AdoMet inhibits endogenous HEK 293 demethylase activity, we extracted demethylase from HEK 293 cells using Q-Sepharose fractionation as previously described (27) and incubated it with increasing concentrations of AdoMet. The results shown in Fig. 5*C* indicate that, similar to recombinant MBD2/dMTase, the demethylase activity extracted from HEK 293 cells is inhibited by 50% at 0.5 mM AdoMet. Taken together, the above experiments demonstrate that AdoMet can inhibit the *in vitro* demethylation activity of recombinant MBD2/dMTase as well as endogenous demethylase extracted from HEK 293 cells.

AdoMet and AdoHcy compete for binding to the catalytic site on DNMTs. It was therefore proposed that the ratio of AdoHcy to AdoMet determines DNMT activity as discussed in the Introduction. AdoHcy inhibits DNMTs whereas increased AdoMet offsets this inhibition. We therefore determined whether a similar relationship applies to MBD2/dMTase. A competition experiment between AdoMet and AdoHcy is presented in Fig. 5*D*. Increasing concentrations of AdoHcy were added in the presence of an inhibitory concentration of AdoMet (10 mM), in a series of demethylation reactions. The results of this experiment illustrate that even a 10-fold concentration excess of AdoHcy to AdoMet does not diminish inhibition of the demethylase reaction by AdoMet. This is consistent with the hypothesis that AdoMet has a higher affinity for MBD2/dMTase as compared with AdoHcy. Further studies are necessary to elucidate the mode of inhibition: whether AdoMet is a competitive inhibitor with the substrate DNA or an allosteric

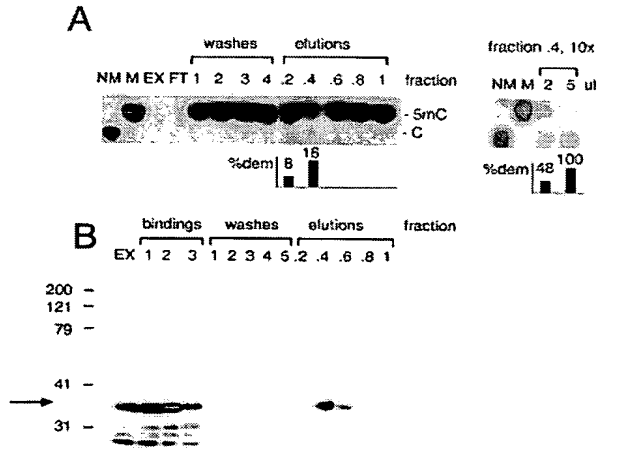

FIG. 4. **Partial purification of His-MBD2/dMTase from Sf9 cells.** *A*, nuclear extracts of Sf9 cells infected with MBD2/dMTase baculovirus were subjected to chromatography on Q-Sepharose and eluted with a stepwise gradient of NaCl. Fractions were assayed for demethylase activity using a ^{32}P-prelabeled methylated DNA from *M. leisodeikticus*. Demethylation activity elutes almost exclusively at 0.4 M NaCl with some activity present in the 0.2 M NaCl fraction (*A*, *left panel*). The 0.4 M NaCl fraction was concentrated 10-fold and re-assayed (*A*, *right panel*). Following demethylation, the DNA was digested to 3′-mononucleotides that were separated by thin layer chromatography. The DNA incubated with the whole cell extract (*EX*) and the flow-through (*FT*) could not be recovered for activity analysis, most likely because of nuclease activities in the fractions. The MBD2/dMTase tightly binds to Q-Sepharose as shown by the fact that the washes are free of demethylation activity. *B*, the fractions were analyzed by Western blot using anti-Xpress antibody (Invitrogen) to demonstrate the presence of His-MBD2/dMTase (indicated by the *arrow*). The presence of the protein correlates with its activity in the elution profile, with almost all MBD2/dMTase detected at 0.4 M NaCl. Lower molecular weight bands in the extract and the bindings might be because of partial degradation of the protein during purification. *NM*, unmethylated control; *M*, methylated control; *5mC*, 5-methyldeoxycytidine 3′-monophosphate; *C*, deoxycytidine 3′-monophosphate.

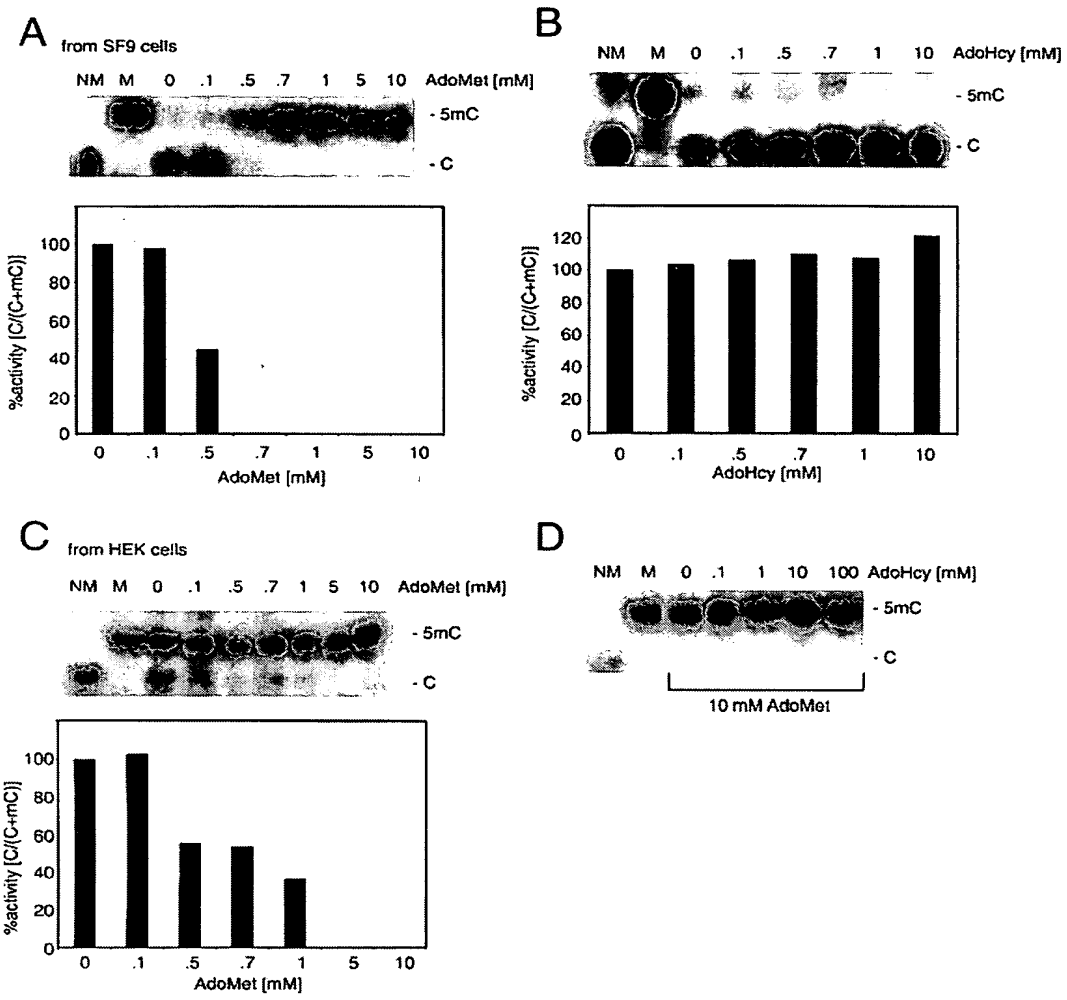

FIG. 5. **AdoMet, but not AdoHcy, inhibits demethylation activity *in vitro*.** *A* and *C*, ^{32}P-prelabeled methylated DNA from *M. leisodeikticus* was incubated with either MBD2/dMTase (*A*) or HEK 293 cells' extracted demethylase (*C*) and increasing concentrations of AdoMet. The autoradiography and quantification of one representative TLC plate is shown. Percent activity was calculated as described under "Materials and Methods." *B*, increasing concentrations of AdoHcy were added to the demethylase reaction; a representative experiment is shown. *D*, increasing concentrations of AdoHcy were added to reaction mixtures containing 10 mM AdoMet and demethylase activity was determined. *NM*, unmethylated control; *M*, methylated control; *5mC*, 5-methyldeoxycytidine 3′-monophosphate; *C*, deoxycytidine 3′-monophosphate.

inhibitor as was demonstrated for methylene tetrahydrofolate reductase (39). Furthermore, we do not know how MBD2/dMTase recognizes AdoMet on a structural basis.

DISCUSSION

The currently accepted mechanism for the effects of the methyl donor AdoMet on DNA methylation and tumorigenesis is founded on the assumption that the DNA methylation reaction is irreversible and defined exclusively by the DNMT. Taking advantage of our previously developed assay of demethylase activity in living cells (Fig. 1), we tested an alternative hypothesis: that AdoMet inhibits demethylase activity. If the steady state methylation status of DNA is maintained by an equilibrium of DNMT and demethylase activities (29), then inhibition of the demethylase side of the equilibrium should result in hypermethylation. Therefore, the reported DNA hypermethylation effects of exogenous AdoMet might be caused in part by inhibiting the level of demethylase activity in tumor cells. The main advantage of the system used in this paper is that it studies active demethylation exclusively, without interference from either replication-dependent passive demethylation or *de novo* DNMT activities (30).

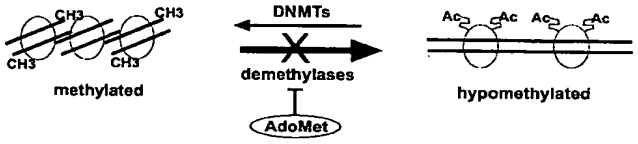

FIG. 6. **Possible model depicting how AdoMet may alter DNA methylation patterns and exert a chemoprotective effect.** The steady state methylation pattern of a gene is determined by an equilibrium of DNMTs and DNA demethylases acting upon it. In cells where DNA demethylase is overexpressed, certain genes may have a tendency to become hypomethylated, and some of these genes may promote anchorage independent growth and tumorigenesis. In this case, the administration of AdoMet would have a tumor protective effect by inhibiting demethylation and shifting the equilibrium to the normally methylated state.

We show here that exogenous AdoMet inhibits TSA-stimulated demethylation of ectopically methylated and transiently

transfected CMV-GFP DNA (Fig. 2, *B* and *E*). Because methylation inhibits the expression of CMV-GFP (30), inhibition of demethylation of CMV-GFP results in reduction of GFP protein expression (Fig. 3, *A* and *C*), illustrating that AdoMet affects both demethylation of DNA and gene expression. This association of inhibition of demethylation and silencing of gene expression prompted us to rule out the possibility that AdoMet has a general, methylation-independent inhibitory effect on gene expression, or a general toxic effect, which also might result in inhibition of expression.

It is possible that AdoMet increases histone methyltransferase activity, resulting in hypermethylation of Lys-9 on H3 histones, which has been shown to correlate with inhibition of acetylation (40, 41). Inhibition of acetylation was shown to inhibit expression and demethylation of CMV-GFP (31). To address this alternative possibility, we measured in parallel the effects that AdoMet might have on methylated as well as unmethylated CMV-GFP plasmid, both transfected and treated with exogenous AdoMet under equivalent conditions. We first show that AdoMet treatment does not result in *de novo* methylation of unmethylated CMV-GFP (Fig. 2*E*). Thus, exogenous AdoMet does not stimulate DNA methylation as might be predicted by the current hypothesis of the mechanism of action of AdoMet. Second, we show that exogenous AdoMet does not inhibit expression of unmethylated CMV-GFP under conditions where a clear inhibition of expression of methylated CMV-GFP is observed (Fig. 3, *B* and *D*). Thus AdoMet specifically affects the expression of methylated genes. To our knowledge, this is the first demonstration that AdoMet specifically targets methylated DNA. This result also rules out the possibility that AdoMet exerts a general toxic effect on the cell. Our data therefore demonstrate that exogenous AdoMet specifically affects methylated DNA and prevents its expression. This most probably occurs by inhibiting an endogenous demethylase activity, resulting in hypermethylation of CMV-GFP and methylation-dependent repression.

We used the product of AdoMet-dependent methyltransferase reactions, AdoHcy, as a control. AdoHcy differs from AdoMet by a single methyl group. We show that AdoHcy has no effect on either gene expression (Fig. 3, *A* and *C*) or demethylation (Fig. 2, *B* and *E*). Taken together, these results indicate that both activities of AdoMet, inhibition of demethylation and inhibition of gene expression, are tightly associated and that they are both dependent on the methyl moiety in AdoMet.

In addition, we show that AdoMet directly inhibits recombinant MBD2/dMTase as well as demethylase activity extracted from HEK 293 cells (Fig. 4) in a dose-dependent manner using an *in vitro* assay (Fig. 5). AdoHcy does not inhibit MBD2/dMTase at the same concentrations (Fig. 5). Because an increase in intracellular AdoHcy was previously shown to be associated with hypomethylation (11), we tested the possibilities that AdoHcy (*a*) stimulates MBD2/dMTase activity, and (*b*) competes with AdoMet binding to MBD2/dMTase and relieves AdoMet inhibition. Our results suggest that AdoHcy does not interact with MBD2/dMTase and that it has no effect on AdoMet inhibition of this enzyme *in vitro*. Our results support the conclusion that the methyl group in AdoMet is required for its interaction with MBD2/dMTase. Although our results demonstrate that exogenous AdoMet inhibits demethylase activity *in vitro* and in living cells, there is no evidence that the intact AdoMet is the inhibitor. Because AdoMet is not intrinsically stable, particularly at physiological pH, it is difficult to assess whether AdoMet or a breakdown product is the inhibitory compound. At the AdoMet concentrations (mM) used in our studies, micromolar or even nanomolar concentrations of breakdown products of AdoMet may be present. Further experiments are required to test this possibility. Nevertheless, our experiments demonstrate that pharmacological administration of AdoMet inhibits active demethylation and alters gene expression.

Further experiments are also required to determine whether MBD2/dMTase is responsible for demethylation of our methylated plasmid in HEK 293 cells. Nevertheless, the fact that AdoMet inhibits both recombinant MBD2/dMTase and endogenous demethylase activities (Fig. 5) provides support for the hypothesis that demethylase(s) is inhibited by AdoMet. Thus, in addition to its role as a cofactor of transmethylation reactions, AdoMet can also act as a regulator of DNA methylation metabolism by inhibiting demethylase activity.

Our data further emphasize that the demethylase side of the methylation equilibrium has to be taken into account when dissecting the mechanism of action of drugs that modify the DNA methylation pattern. Based on our data, we suggest that AdoMet can alter DNA methylation patterns by inhibiting demethylase, which is expressed in some or most cells (Fig. 6). In this case, a reduction in the intracellular levels of AdoMet by methyl-deficient diets removes this inhibition and increases the demethylase tone, resulting in active demethylation of DNA that could take place even in postmitotic tissue. Interestingly, AdoMet has recently been shown to inhibit the overall demethylation of a CG site in the 5′ of the myogenin gene during C2C12 differentiation (21). However, this report did not determine whether AdoMet stimulated DNMT or inhibited DNA demethylase.

What are the potential implications of the inhibition of demethylase by AdoMet? It is well documented that a correlation exists between reduced intracellular AdoMet (either as a consequence of decreased folate intake or pharmacological intervention) and an increase in cell proliferation and tumorigenesis (6, 35, 36, 38). In addition, other studies have shown that a decrease in dietary folate, or a depletion of intracellular AdoMet, results in DNA hypomethylation (6, 12, 36, 37). This is consistent with the well documented observations of global hypomethylation in cancer cells (42). There is evidence that the tumor protective mechanism of AdoMet involves DNA methylation because this protection is removed when the animals are co-treated with 5-azacytidine and AdoMet (19). In accordance with this hypothesis, we have recently shown that antisense inhibition of MBD2/demethylase inhibits tumorigenesis (43). It is tempting to speculate that certain genes that are required for anchorage independent growth might be inhibited by methylation and activated by demethylase activity. Inhibition of the demethylase tone by AdoMet is proposed to result in silencing of these genes. If the mechanism of action of AdoMet in inhibiting tumorigenesis involves inhibition of demethylation, it would support the hypothesis that demethylation plays a causal role in tumorigenesis, and serve as a warning against using inhibitors of DNA methylation as anticancer agents.

Acknowledgment—We thank Johanne Theberge for excellent technical help and support.

REFERENCES

1. Lu, S. C. (2000) *Int. J. Biochem. Cell Biol.* **32**, 391–395
2. Finkelstein, J. D. (2000) *Semin. Thromb. Hemostasis* **26**, 219–225
3. Potter, J. D. (2002) *J. Nutr.* **132**, 2410S–2412S
4. Mato, J. M., Alvarez, L., Ortiz, P., and Pajares, M. A. (1997) *Pharmacol. Ther.* **73**, 265–280
5. Poirier, L. A. (2002) *J. Nutr.* **132**, 2336S–2339S
6. Pascale, R., Simile, M., De, M. M., and Feo, F. (2002) *Alcohol* **27**, 193–198
7. Cheng, X., and Roberts, R. J. (2001) *Nucleic Acids Res.* **29**, 3784–3795
8. Chiang, P. K., Gordon, R. K., Tal, J., Zeng, G. C., Doctor, B. P., Pardhasaradhi, K., and McCann, P. P. (1996) *FASEB J.* **10**, 471–480
9. Chiang, P. K. (1998) *Pharmacol. Ther.* **77**, 115–134
10. Garcea, R., Daino, L., Pascale, R., Simile, M. M., Puddu, M., Ruggiu, M. E.,

Seddaiu, M. A., Satta, G., Sequenza, M. J., and Feo, F. (1989) *Carcinogenesis* **10,** 1183–1192
11. Caudill, M. A., Wang, J. C., Melnyk, S., Pogribny, I. P., Jernigan, S., Collins, M. D., Santos-Guzman, J., Swendseid, M. E., Cogger, E. A., and James, S. J. (2001) *J. Nutr.* **131,** 2811–2818
12. Pogribny, I. P., Poirier, L. A., and James, S. J. (1995) *Carcinogenesis* **16,** 2863–2867
13. Steinmetz, K. L., Pogribny, I. P., James, S. J., and Pitot, H. C. (1998) *Carcinogenesis* **19,** 1487–1494
14. Stern, L. L., Mason, J. B., Selhub, J., and Choi, S. W. (2000) *Cancer Epidemiol. Biomarkers Prev.* **9,** 849–853
15. Friso, S., Choi, S. W., Girelli, D., Mason, J. B., Dolnikowski, G. G., Bagley, P. J., Olivieri, O., Jacques, P. F., Rosenberg, I. H., Corrocher, R., and Selhub, J. (2002) *Proc. Natl. Acad. Sci. U. S. A.* **99,** 5606–5611
16. Ehrlich, M. (2002) *J. Nutr.* **132,** 2424S-2429S
17. Feinberg, A. P., Gehrke, C. W., Kuo, K. C., and Ehrlich, M. (1988) *Cancer Res.* **48,** 1159–1161
18. Jones, P. A., and Taylor, S. M. (1980) *Cell* **20,** 85–93
19. Pascale, R., Simile, M. M., Ruggiu, M. E., Seddaiu, M. A., Satta, G., Sequenza, M. J., Daino, L., Vannini, M. G., Lai, P., and Feo, F. (1991) *Cancer Lett.* **56,** 259–265
20. Watson, W. H., Zhao, Y., and Chawla, R. K. (1999) *Biochem. J.* **342,** 21–25
21. Fuso, A., Cavallaro, R. A., Orru, L., Buttarelli, F. R., and Scarpa, S. (2001) *FEBS Lett.* **508,** 337–340
22. Oswald, J., Engemann, S., Lane, N., Mayer, W., Olek, A., Fundele, R., Dean, W., Reik, W., and Walter, J. (2000) *Curr. Biol.* **10,** 475–478
23. Ramchandani, S., Bhattacharya, S. K., Cervoni, N., and Szyf, M. (1999) *Proc. Natl. Acad. Sci. U. S. A.* **96,** 6107–6112
24. Bhattacharya, S. K., Ramchandani, S., Cervoni, N., and Szyf, M. (1999) *Nature* **397,** 579–583
25. Ng, H. H., Zhang, Y., Hendrich, B., Johnson, C. A., Turner, B. M., Erdjument-Bromage, H., Tempst, P., Reinberg, D., and Bird, A. (1999) *Nat. Genet.* **23,** 58–61
26. Zhang, Y., Ng, H. H., Erdjument-Bromage, H., Tempst, P., Bird, A., and Reinberg, D. (1999) *Genes Dev.* **13,** 1924–1935
27. Detich, N., Theberge, J., and Szyf, M. (2002) *J. Biol. Chem.* **277,** 35791–35794
28. Szyf, M. (2001) *Trends Pharmacol. Sci.* **22,** 350–354
29. Szyf, M. (2001) *Front. Biosci.* **6,** D599–D609
30. Cervoni, N., and Szyf, M. (2001) *J. Biol. Chem.* **276,** 40778–44087
31. Cervoni, N., Detich, N., Seo, S. B., Chakravarti, D., and Szyf, M. (2002) *J. Biol. Chem.* **277,** 25026–25031
32. Rouleau, J., Tanigawa, G., and Szyf, M. (1992) *J. Biol. Chem.* **267,** 7368–7377
33. Szyf, M., and Bhattacharya, S. K. (2002) *Methods Mol. Biol.* **200,** 155–161
34. Deleted in proof
35. Cai, J., Mao, Z., Hwang, J. J., and Lu, S. C. (1998) *Cancer Res.* **58,** 1444–1450
36. Sibani, S., Melnyk, S., Pogribny, I. P., Wang, W., Hiou-Tim, F., Deng, L., Trasler, J., James, S. J., and Rozen, R. (2002) *Carcinogenesis* **23,** 61–65
37. Zhao, C. Q., Young, M. R., Diwan, B. A., Coogan, T. P., and Waalkes, M. P. (1997) *Proc. Natl. Acad. Sci. U. S. A.* **94,** 10907–10912
38. Martinez-Chantar, M. L., Corrales, F. J., Martinez-Cruz, L. A., Garcia-Trevijano, E. R., Huang, Z. Z., Chen, L., Kanel, G., Avila, M. A., Mato, J. M., and Lu, S. C. (2002) *FASEB J.* **16,** 1292–1294
39. Jencks, D. A., and Mathews, R. G. (1987) *J. Biol. Chem.* **262,** 2485–2493
40. Dillon, N., and Festenstein, R. (2002) *Trends Genet.* **18,** 252–258
41. Nakayama, J., Rice, J. C., Strahl, B. D., Allis, C. D., and Grewal, S. I. (2001) *Science* **292,** 110–113
42. Ehrlich, M. (2002) *Oncogene* **21,** 5400–5413
43. Slack, A., Bovenzi, V., Bigey, P., Ivanov, M. A., Ramchandani, S., Bhattacharya, S., TenOever, B., Lamrihi, B., Scherman, D., and Szyf, M. (2002) *J. Gene. Med.* **4,** 381–389

Proc. Natl. Acad. Sci. USA
Vol. 93, pp. 9821–9826, September 1996
Medical Sciences

Methylation-specific PCR: A novel PCR assay for methylation status of CpG islands

(DNA methylation/tumor suppressor genes/*p16*/*p15*)

JAMES G. HERMAN*†, JEREMY R. GRAFF*, SANNA MYÖHÄNEN*, BARRY D. NELKIN*, AND STEPHEN B. BAYLIN*‡

*Oncology Center and ‡Department of Medicine, The Johns Hopkins Medical Institutions, 424 North Bond Street, Baltimore, MD 21231

Communicated by Victor A. McKusick, Johns Hopkins Hospital, Baltimore, MD, June 3, 1996 (received for review April 3, 1996)

ABSTRACT **Precise mapping of DNA methylation patterns in CpG islands has become essential for understanding diverse biological processes such as the regulation of imprinted genes, X chromosome inactivation, and tumor suppressor gene silencing in human cancer. We describe a new method, MSP (methylation-specific PCR), which can rapidly assess the methylation status of virtually any group of CpG sites within a CpG island, independent of the use of methylation-sensitive restriction enzymes. This assay entails initial modification of DNA by sodium bisulfite, converting all unmethylated, but not methylated, cytosines to uracil, and subsequent amplification with primers specific for methylated versus unmethylated DNA. MSP requires only small quantities of DNA, is sensitive to 0.1% methylated alleles of a given CpG island locus, and can be performed on DNA extracted from paraffin-embedded samples. MSP eliminates the false positive results inherent to previous PCR-based approaches which relied on differential restriction enzyme cleavage to distinguish methylated from unmethylated DNA. In this study, we demonstrate the use of MSP to identify promoter region hypermethylation changes associated with transcriptional inactivation in four important tumor suppressor genes (*p16*, *p15*, *E-cadherin*, and von Hippel-Lindau) in human cancer.**

In higher order eukaryotes, DNA is methylated only at cytosines located 5′ to guanosine in the CpG dinucleotide (1). This modification has important regulatory effects on gene expression, especially when involving CpG-rich areas known as CpG islands, located in the promoter regions of many genes (2, 3). While almost all gene-associated islands are protected from methylation on autosomal chromosomes (3), extensive methylation of CpG islands has been associated with transcriptional inactivation of selected imprinted genes (4, 5) and genes on the inactive X-chromosome of females (6, 7). Aberrant methylation of normally unmethylated CpG islands has been documented as a relatively frequent event in immortalized and transformed cells (8) and has been associated with transcriptional inactivation of defined tumor suppressor genes in human cancers (9–12). In this last situation, promoter region hypermethylation stands as an alternative to coding region mutations in eliminating tumor suppressor gene function (9, 10). Therefore, mapping of methylation patterns in CpG islands has become an important tool for understanding both normal and pathologic gene expression events.

Mapping of methylated regions in DNA has relied primarily on Southern hybridization approaches, based on the inability of methylation-sensitive restriction enzymes to cleave sequences that contain one or more methylated CpG sites. This method provides an assessment of the overall methylation status of CpG islands, including some quantitative analysis (13), but requires large amounts of high molecular weight DNA (generally 5 μg or more), can detect methylation only if present in greater than a few percent of the alleles and can only provide information about those CpG sites found within sequences recognized by methylation-sensitive restriction enzymes. A more sensitive method of methylation detection combines the use of methylation-sensitive enzymes and PCR (14). After digestion of DNA with the enzyme, PCR will amplify from primers flanking the restriction site only if DNA cleavage has been prevented by methylation (15, 16). Like Southern-based approaches, this method can only monitor CpG methylation in methylation-sensitive restriction sites. Moreover, the restriction of unmethylated DNA must be complete, since any uncleaved DNA will be amplified by PCR yielding a false positive result for methylation. This approach has been useful in studying samples where a high percentage of alleles of interest are methylated, such as the study of imprinted genes (5, 15, 16) and X chromosome-inactivated genes (14). However, difficulties in distinguishing between incomplete restriction and low numbers of methylated alleles make this approach unreliable for detection of tumor suppressor gene hypermethylation in small samples or in samples where methylated alleles represent a small fraction of the population.

The chemical modification of cytosine to uracil by bisulfite treatment has provided another method for the study of DNA methylation that avoids the use of restriction enzymes (17). In this reaction, all cytosines are converted to uracil, but those that are methylated (5-methylcytosine) are resistant to this modification and remain as cytosine (18). This altered DNA can then be amplified and sequenced, providing detailed information within the amplified region of the methylation status of all CpG sites (17). However, this method is technically rather difficult and labor-intensive, and, without cloning of the amplified products, the technique is less sensitive than Southern analysis, requiring ≈25% of the alleles to be methylated for detection (19).

We now report a novel PCR method, methylation-specific PCR (MSP), which is sensitive and specific for methylation of virtually any block of CpG sites in a CpG island. We designed primers to distinguish methylated from unmethylated DNA in bisulfite-modified DNA, taking advantage of the sequence differences resulting from bisulfite modification. Unmodified DNA or DNA incompletely reacted with bisulfite can also be distinguished, since marked sequence differences exist between these DNAs. The frequency of CpG sites in CpG islands renders this technique uniquely useful and extremely sensitive for such regions. Herein, we detail the MSP procedure and show its use for detecting the aberrant methylation of four tumor suppressor genes in human neoplasia.

MATERIALS AND METHODS

DNA and Cell Lines. Genomic DNA was obtained from cell lines, primary tumors, and normal tissue as described (10–12).

The publication costs of this article were defrayed in part by page charge payment. This article must therefore be hereby marked "*advertisement*" in accordance with 18 U.S.C. §1734 solely to indicate this fact.

Abbreviations: MSP, methylation-specific PCR; *VHL*, von Hippel-Lindau.

†To whom reprint requests should be addressed.

The renal carcinoma cell line was kindly provided by Michael Lerman (National Cancer Institute, Frederick, MD).

Bisulfite Modification. DNA (1 μg) in a volume of 50 μl was denatured by NaOH (final concentration, 0.2 M) for 10 min at 37°C. For samples with nanogram quantities of human DNA, 1 μg of salmon sperm DNA (Sigma) was added as carrier before modification. Thirty microliters of 10 mM hydroquinone (Sigma) and 520 μl of 3 M sodium bisulfite (Sigma) at pH 5, both freshly prepared, were added and mixed, and samples were incubated under mineral oil at 50°C for 16 hr. Modified DNA was purified using the Wizard DNA purification resin according to the manufacturer (Promega) and eluted into 50 μl of water. Modification was completed by NaOH (final concentration, 0.3 M) treatment for 5 min at room temperature, followed by ethanol precipitation. DNA was resuspended in water and used immediately or stored at −20°C.

Genomic Sequencing. Genomic sequencing of bisulfite-modified DNA (17) was accomplished using the solid-phase DNA sequencing approach (19). Bisulfite modified DNA (100 ng) was amplified with *p16* gene-specific primers 5′-TTTTTAGAGGATTTGAGGGATAGG (sense) and 5′-CTACCTAATTCCAATTCCCCTACA (anti-sense). PCR conditions were as follows: 96°C for 3 min and 80°C for 3 min, after which 1 unit of *Taq* polymerase (BRL) was added; then 35 cycles of 96°C for 20 sec, 56°C for 20 sec, 72°C for 90 sec; and finally 5 min at 72°C. The PCR mixture contained 1× buffer (BRL) with 1.5 mM $MgCl_2$, 20 pmol of each primer, and 0.2 mM dNTPs. To obtain products for sequencing, a second round of PCR was performed with 5 pmol of nested primers. In this reaction, the sense primer, 5′-GTTTTCCCAGTCACGACAGTATTAGGAGGAAGAAAGAGGAG, contains M13-40 sequence (underlined) introduced as a site to initiate sequencing, and the anti-sense primer 5′-TCCAATTCCCCTACAAACTTC is biotinylated to facilitate purification of the product before sequencing. PCR was performed as above, for 32 cycles with 2.5 mM $MgCl_2$. All primers for genomic sequencing were designed to avoid any CpGs in the sequence. Biotinylated PCR products were purified using streptavidin-coated magnetic beads (Dynal, Oslo), and sequencing reactions were performed with Sequenase and M13-40 sequencing primer under conditions specified by the manufacturer (United States Biochemical).

PCR Amplification. Primer pairs described in Table 1 (20–24) were purchased from Life Technologies. The PCR mixture contained 1× PCR buffer (16.6 mM ammonium sulfate/67 mM Tris, pH 8.8/6.7 mM $MgCl_2$/10 mM 2-mercaptoethanol), dNTPs (each at 1.25 mM), primers (300 ng each per reaction), and bisulfite-modified DNA (≈50 ng) or unmodified DNA (50–100 ng) in a final volume of 50 μl. PCR specific for unmodified DNA also included 5% dimethyl sulfoxide. Reactions were hot-started at 95°C for 5 min before the addition of 1.25 units of *Taq* polymerase (BRL). Amplification was carried out in a Hybaid OmniGene temperature cycler for 35 cycles (30 sec at 95°C, 30 sec at the annealing temperature listed in Table 1, and 30 sec at 72°C), followed by a final 4-min extension at 72°C. Controls without DNA were performed for each set of PCRs. Each PCR (10 μl) was directly loaded onto nondenaturing 6–8% polyacrylamide gels, stained with ethidium bromide, and directly visualized under UV illumination.

Restriction Analysis. Of the 50 μl of PCR mixture, 10 μl was digested with 10 units of *Bst*UI (New England Biolabs) for 4 hr, according to conditions specified by the manufacturer. Restriction digests were ethanol precipitated before gel analysis.

RESULTS

Validating the Design Strategy for MSP: Genomic Sequencing of *p16*. An initial study was required to validate whether our strategy for MSP would prove feasible for assessing the methylation status of CpG islands. We needed to determine whether the density of methylation, in key regions to be tested, was great enough to facilitate our primer design. We chose to test this for the *p16* tumor suppressor gene in which we (10, 25) and others (26, 27) have documented that hypermethylation of a 5′ CpG island is associated with complete loss of gene expression in many cancer types. However, other than for CpG sites located in recognition sequences for methylation-sensitive enzymes, the density of methylation and its correlation to transcriptional silencing has not been established. We thus employed the genomic sequencing technique to explore this relationship. As has been found for other CpG islands examined in this manner (19, 28, 29), the CpG island of *p16* had no methylation at any CpG site in those cell lines and normal tissues previously found to be unmethylated by Southern analysis (Fig. 1; refs. 10 and 25). However, it was extensively methylated in cancer cell lines shown to be methylated by Southern analysis (Fig. 1). In fact, all cytosines within CpG dinucleotides in this region were completely methylated in the cancers lacking *p16* transcription. This marked difference in sequence following bisulfite treatment suggested that our

Table 1. PCR primers used for MSP

Primer set	Sense primer,* 5′ → 3′	Antisense primer,* 5′ → 3′	Size, bp	Anneal temp., °C	Genomic position†
p16-W‡	CAGAGGGTGGGGCGGACCGC	CGGGCCGCGGCCGTGG	140	65	+171
p16-M	TTATTAGAGGGTGGGGCGGATCGC	GACCCCGAACCGCGACCGTAA	150	65	+167
p16-U	TTATTAGAGGGTGGGGTGGATTGT	CAACCCCAAACCACAACCATAA	151	60	+167
p16-M2	TTATTAGAGGGTGGGGCGGATCGC	CCACCTAAATCGACCTCCGACCG	234	65	+167
p16-U2	TTATTAGAGGGTGGGGTGGATTGT	CCACCTAAATCAACCTCCAACCA	234	60	+167
p15-W	CGCACCCTGCGGCCAGA	AGTGGCCGAGCGGCCGG	137	65	+46
p15-M	GCGTTCGTATTTTGCGGTT	CGTACAATAACCGAACGACCGA	148	60	+40
p15-U	TGTGATGTGTTTGTATTTTGTGGTT	CCATACAATAACCAAACAACCAA	154	60	+34
VHL-M	TGGAGGATTTTTTTGCGTACGC	GAACCGAACGCCGCGAA	158	60	−116
VHL-U	GTTGGAGGATTTTTTTGTGTATGT	CCCAAACCAAACACCACAAA	165	60	−118
Ecad-M	TTAGGTTAGAGGGTTATCGCGT	TAACTAAAAATTCACCTACCGAC	116	57	−205
Ecad-U	TAATTTTAGGTTAGAGGGTTATTGT	CACAACCAATCAACAACACA	97	53	−210

*Sequence differences between modified primers and unmodified DNA are in boldface type and differences between methylated/modified and ummethylated/modified are underlined.

†Primers were placed near the transcriptional start site. Genomic position is the location of the 5′ nucleotide of the sense primer in relation to the major transcriptional start site defined in the following references and Genbank accession numbers: *p16* (most 3′ site), X94154 (20); *p15*, S75756 (22); *VHL*, U19763 (23); and *E-cadherin*, L34545 (24).

‡W represents unmodified or wild-type primers. M, methylated-specific primers; and U, unmethylated-specific primers.

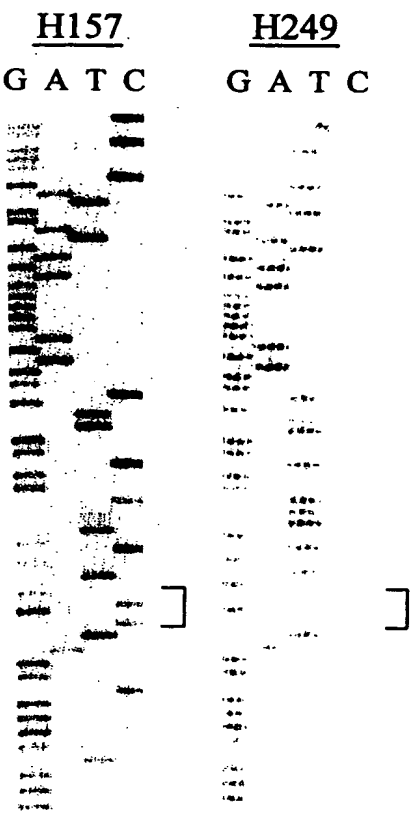

FIG. 1. Genomic sequencing of *p16*. The sequence shown has the most 5′ region at the bottom of the gel, beginning at +175 in relation to a major transcriptional start site (20). All cytosines in the unmethylated cell line H249 have been converted to thymidine, while all Cs in CpG dinucleotides in the methylated cell H157 remain as C, indicating methylation. Designated by the bracket (]) is a *Bst*UI site, which is at −59 in relation to the translational start site in GenBank sequence U12818 (21), but which is incorrectly identified as CGAG in sequence X94154 (20). This CGCG site represents the 3′ location of the sense primer used for *p16* MSP.

strategy for specific amplification of either methylated or unmethylated alleles was feasible.

Primer Design for MSP. Primers were designed to discriminate between methylated and unmethylated alleles following bisulfite treatment and to discriminate between DNA modified by bisulfite and that which had not been modified. To accomplish this, primer sequences were chosen for regions containing frequent cytosines (to distinguish unmodified from modified DNA), and CpG pairs near the 3′ end of the primers (to provide maximal discrimination in the PCR between methylated and unmethylated DNA). Since the two strands of DNA are no longer complementary after bisulfite treatment, primers can be designed for either modified strand. For convenience, we have designed primers for the sense strand. The fragment of DNA to be amplified was intentionally small, to allow the assessment of methylation patterns in a limited region and to facilitate the application of this technique to samples, such as paraffin blocks, where amplification of larger fragments is not possible. In Table 1, primer sequences are shown for all genes tested, emphasizing the differences in sequence between the three types of DNA that are exploited for the specificity of MSP. The multiple mismatches in these primers, which are specific for these different types of DNA, suggest that each primer set should provide amplification only from the intended template.

MSP Analysis of *p16*. We first tested the primers designed for *p16* on DNA from cancer cell lines and normal tissues for which the methylation status had previously been defined by Southern analysis (10, 25). In all cases, the primer set used confirmed the methylation status determined by Southern analysis. For example, lung cancer cell lines U1752 and H157, as well as other cell lines with methylated *p16* alleles, amplified only with the methylated primers (Fig. 2*A*). DNA from normal tissues (lymphocytes, lung, kidney, breast, and colon) and the lung cancer cell lines H209 and H249, having only unmethylated *p16* alleles, amplified only with unmethylated primers (examples in Fig. 2*A*). PCR with these primers could be performed with or without 5% dimethyl sulfoxide. DNA not treated with bisulfite (unmodified) failed to amplify with either set of methylated or unmethylated specific primers, but readily amplified with primers specific for the sequence before modification (Fig. 2*A*). DNA from the cell line H157 after bisulfite treatment also produced a weak amplification with unmodified primers, suggesting an incomplete bisulfite reaction. We have occasionally observed this in other samples. However, this unmodified DNA, unlike partially restricted DNA in previous PCR assays relying on methylation-sensitive restriction enzymes, is not recognized by the primers specific for modified DNA. It therefore does not provide a false positive result or interfere with the ability to distinguish methylated from unmethylated alleles.

We next sought to define the sensitivity of MSP for detection of methylated *p16* alleles. DNA from cell lines with methylated *p16* alleles was mixed with DNA with unmethylated *p16* alleles before bisulfite treatment. We could consistently detect 0.1% of methylated DNA (≈50 pg) present in an otherwise unmethylated sample (Fig. 2*B*). We have also determined the sensitivity limit for the amount of input DNA. As little as 1 ng of human DNA, mixed with salmon sperm DNA as a carrier, was detectable by MSP (data not shown).

Fresh human tumor samples often contain normal and tumor tissue, making the detection of changes specific for the tumor difficult. However, the sensitivity of MSP suggests it would be useful for primary tumors as well, allowing for detection of aberrantly methylated alleles even if they contribute relatively little to the overall DNA in a sample. In each case, while normal tissues (lymphocytes, lung, kidney, and colon) were unmethylated at the *p16* locus, tumors found to be methylated at the *p16* CpG island by Southern analysis also contained methylated DNA detected by MSP, in addition to some unmethylated alleles (examples in Fig. 2*B*). Analysis of DNA from paraffin-embedded tumors revealed methylated and unmethylated alleles (example in Fig. 2*B*), as shown for the same primary lung cancer in Fig. 2*B*. To confirm that these results were not unique to this primer set, we used a second downstream primer for *p16* that would amplify a slightly larger fragment (Table 1). This second set of primers reproduced the results described above (Fig. 2*C*), confirming the methylation status defined by Southern blot analysis.

To verify further the specificity of the primers for the methylated alleles and to check specific cytosines for methylation within the region amplified, we took advantage of the differences in sequence at a methylation-sensitive restriction site between methylated/modified DNA and unmethylated/modified DNA. Specifically, the *Bst*UI recognition site, CGCG, will remain CGCG if both Cs are methylated after bisulfite treatment and amplification but will become TGTG if unmethylated. Digestion of the amplified products with *Bst*UI will then distinguish these two products, as restriction of *p16* amplified products illustrates. Only unmodified products and methylated/modified products, both of which retain the

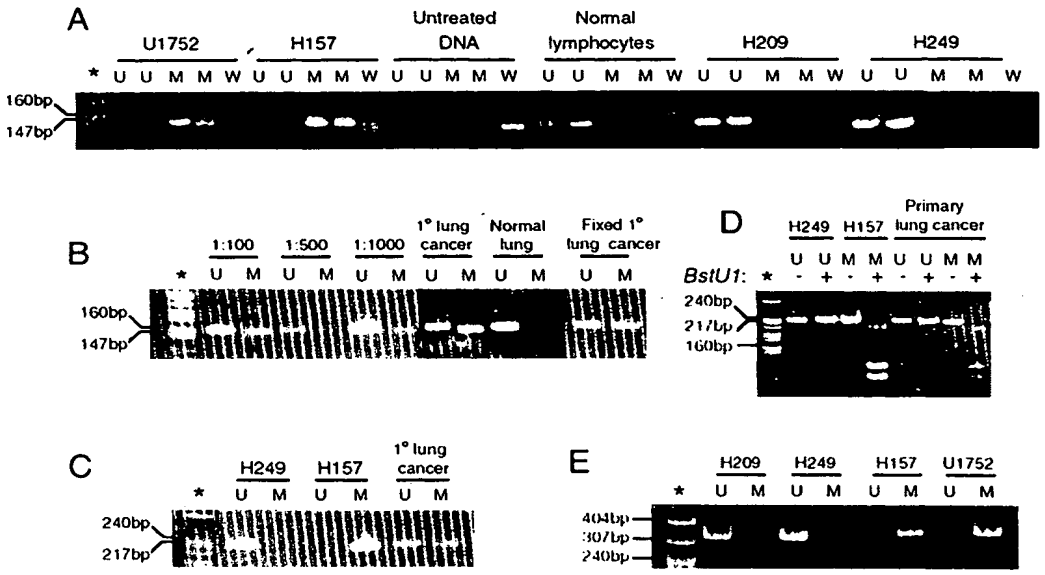

FIG. 2. MSP of *p16*. Primer sets used for amplification are designated as unmethylated (U), methylated (M), or unmodified/wild-type (W). *, Molecular weight marker pBR322-*Msp*I digest. (*A*) Amplification of bisulfite-treated DNA from cancer cell lines and normal lymphocytes, and untreated DNA (from cell line H249). (*B*) Mixing of various amounts of H157 DNA with 1 μg of H249 DNA before bisulfite treatment to assess the detection sensitivity of MSP for methylated alleles. Modified DNA from a primary lung cancer sample, normal lung, and the paraffin-embedded (fixed) tissue block of this primary lung cancer are also shown. (*C*) Amplification with the p16-U2 (U) primers, and p16-M2 (M) described in Table 1. (*D*) The amplified *p16* products of *C* were restricted with *Bst*UI (+) or were not restricted (−). (*E*) Testing for regional methylation of CpG islands with MSP, using sense primers p16-U2 (U) and p16-M2 (M), which are methylation-specific, and an antisense primer that is not methylation-specific.

CGCG site, are cleaved by *Bst*UI. Products amplified with unmethylated/modified primers failed to be cleaved (Fig. 2*D*).

The primer sets discussed above were designed to discriminate heavily methylated CpG islands from unmethylated alleles. To do this, both the upper (sense) and lower (antisense) primers contained CpG sites that could produce methylation-dependent sequence differences after bisulfite treatment. MSP might be employed to examine more regional aspects of CpG island methylation. To examine this, we tested whether methylation-dependent differences in the sequence of just one primer would still allow the discrimination between unmethylated and methylated *p16* alleles. The antisense primer used for genomic sequencing, 5′-CTACCTAATTCCAATTCCCCTACA, was used as the antisense primer, which contains no CpG sites, and was paired with either a methylated or unmethylated sense primer (Table 1). Amplification of the predicted 313-bp PCR product only occurred with the unmethylated sense primer in H209 and H249 (unmethylated by Southern) and only with the methylated sense primer in H157 and U1752 (methylated by Southern), indicating that methylation of CpG sites within a defined region can be recognized by specific primers and distinguish between methylated and unmethylated alleles (Fig. 2*E*).

The Use of MSP for the Analysis of Other Genes. We extended our study to include three other genes transcriptionally silenced in human cancers by aberrant hypermethylation of 5′ CpG islands. The cyclin-dependent kinase inhibitor *p15* is aberrantly methylated in many leukemic cell lines and primary leukemias (11). For *p15*, MSP again verified the methylation status determined by Southern analysis. Thus, normal lymphocytes and cancer cell lines SW48 and U1752, containing only unmethylated alleles of *p15* alleles by Southern analysis (11), amplified only with the unmethylated set of primers, while the lung cancer cell line H1618 and leukemia cell line KG1A amplified only with the methylated set of primers (Fig. 3*A*), consistent with previous Southern analysis results (11). DNA from the cell line Raji produced a strong PCR product with methylated primers and a weaker band with unmethylated primers. This was the same result for methylation obtained previously by Southern analysis (11). Noncultured leukemia samples, like the primary tumors studied for *p16*, had amplification with the methylated primer set as well as the unmethylated set. This heterogeneity also matched Southern analysis (11). Again, as for *p16*, differential modification of *Bst*UI restriction sites in the amplified product of *p15* was used to verify the specific amplification by MSP (Fig. 3*B*). Amplified products using methylated primer sets from cell lines H1618 and Raji or unmodified primer sets, were completely cleaved by *Bst*UI, while amplified products from the unmethylated primer set did not cleave. The smaller sizes of products observed in the unmodified product reflect the 11-bp difference in size of the original PCR product. Primary acute myelogenous leukemia samples also demonstrated cleavage only in the methylated product but had less complete cleavage. This suggests a heterogeneity in methylation, where methylation is extensive in the region underlying the methylation-specific primers, allowing amplification by MSP but is not inclusive of all CpG sites between the primers for each allele.

Aberrant CpG island promoter region methylation is associated with inactivation of the von Hippel-Lindau (*VHL*) tumor suppressor gene in ≈20% of clear cell renal carcinomas (9). This event, like mutations for *VHL* (30), is restricted to clear cell renal cancers (9). Primers designed for the *VHL* sequence were used to study DNA from the renal cell cancer cell line RFX393, which is methylated at *VHL* by Southern analysis (data not shown), and DNA from the lung cancer cell line U1752, which is unmethylated at this locus (9). In each case, the methylation status of *VHL* determined by MSP confirmed that found by Southern analysis (Fig. 3*C*), and *Bst*UI restriction site analysis validated the PCR product specificity (Fig. 3*D*).

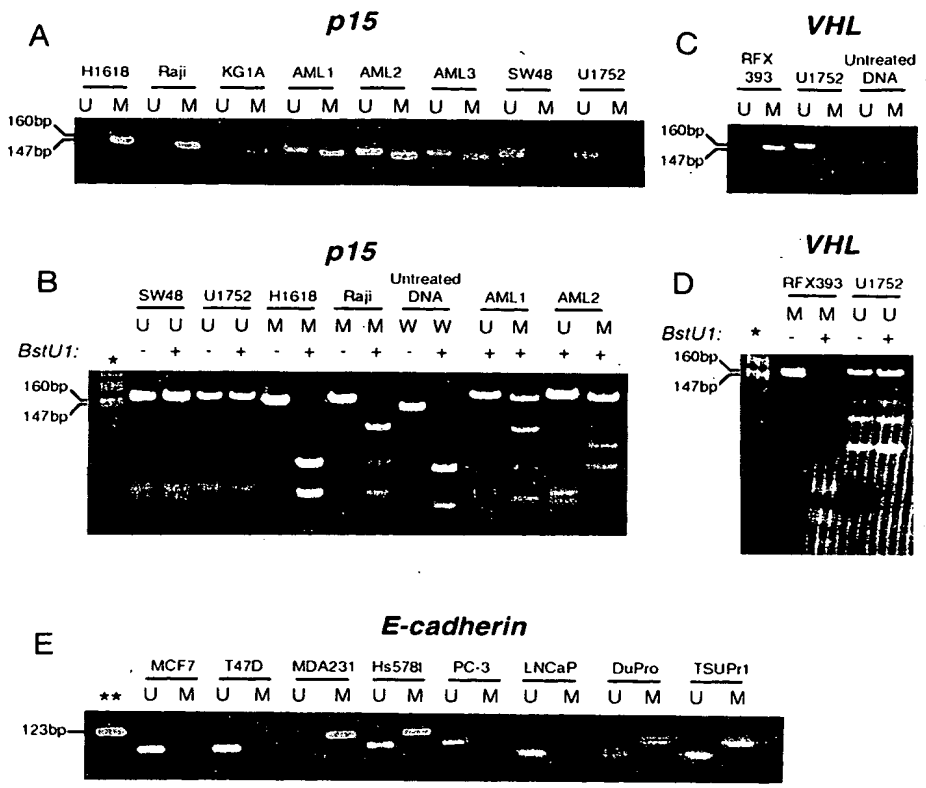

FIG. 3. MSP analysis of several genes. Primer sets used for amplification are designated as unmethylated (U), methylated (M), or unmodified/wild-type (W). *, Molecular weight marker pBR322-*MspI* digest; and **, 123-bp molecular weight marker. All DNA samples were bisulfite-treated except those designated untreated. (*A*) MSP for p15. (*B*) The *p15* products were restricted with *Bst*UI (+) or were not restricted (−). (*C*) MSP for *VHL*. (*D*) The *VHL* products were restricted with *Bst*UI (+) or were not restricted (−). The smaller molecular weight fragments seen in the U lanes represent primer dimers, which are present in lanes without template DNA and can be faintly seen in *C*. (*E*) MSP for *E-cadherin*.

The expression of the invasion/metastasis suppressor gene, *E-cadherin*, is often silenced by aberrant methylation of the 5′ promoter in breast, prostate, and many other carcinomas (12, 31). We designed primers for the *E-cadherin* promoter region to test the use of MSP for this gene. In each case, MSP analysis paralleled Southern blot analysis for the methylation status of the gene (12). DNA from breast cancer cell lines MDA-MB-231, HS578t, and prostate cancer cell lines DuPro, and TSUPr1, all heavily methylated by Southern blot, displayed prominent methylation. DNA from MCF7, T47D, PC-3, and LNCaP, all unmethylated by Southern, showed no evidence for methylation in the sensitive MSP assay (Fig. 3*E*). MSP analysis revealed the presence of unmethylated alleles in Hs578t, TSUPr1, and DuPro, consistent with a low percentage of unmethylated alleles in these cell lines previously detected by Southern analysis (12). *Bst*UI restriction analysis again confirmed the specificity of the PCR amplification (data not shown).

DISCUSSION

We have described a novel PCR approach, MSP, for rapid analysis of the methylation status of CpG islands. As illustrated, this technique provides significant advantages over previous PCR-based techniques and other methods used for assaying methylation. MSP is markedly more sensitive than Southern analysis, facilitating detection of low numbers of methylated alleles and the study of DNA from small samples. MSP allows the study of paraffin-embedded materials, which could not previously be analyzed by Southern analysis. MSP also allows examination of all CpG sites, not just those within sequences recognized by methylation-sensitive restriction enzymes. This markedly increases the number of such sites that can be assessed and will allow rapid, fine mapping of methylation patterns throughout CpG-rich regions. This latter point was demonstrated for *p16*, where the discrimination between methylated and unmethylated alleles could be attributed to differences in methylation in an 8-bp region. MSP also eliminates the frequent false positive results due to partial digestion of methylation-sensitive enzymes inherent in previous PCR methods for detecting methylation. Furthermore, with MSP, simultaneous detection of unmethylated and methylated products in a single sample confirms the integrity of DNA as a template for PCR and allows a semiquantitative assessment of allele types that approximates the quantitation determined by Southern analysis. Finally, the ability to validate the amplified product by differential restriction patterns is an additional advantage.

The only technique that can provide more direct analysis than MSP for most CpG sites within a defined region is genomic sequencing. However, MSP can provide similar information and has the following advantages. First, MSP is much simpler and requires less time than genomic sequencing, with a typical PCR and gel analysis taking 4–6 hr. In contrast, for genomic sequencing, amplification, cloning, and subsequent sequencing may take days. Second, MSP avoids the use of expensive sequencing reagents and the use of radioactivity.

Both of these factors make MSP better suited for the analysis of large numbers of samples. Third, the use of PCR as the step to distinguish methylated from unmethylated DNA in MSP allows for a significant increase in the sensitivity of methylation detection. For example, if cloning is not used before genomic sequencing of the DNA, <10% methylated DNA in a background of unmethylated DNA cannot be seen (19). The use of PCR and cloning does allow sensitive detection of methylation patterns in very small amounts of DNA by genomic sequencing (17, 32). However, in practice, this would require sequencing analysis of 10 clones to detect 10% methylation, 100 clones to detect 1% methylation, and, to reach the level of sensitivity we have demonstrated with MSP (1:1000), one would have to sequence 1000 individual clones.

In summary, MSP is a simple, sensitive, and specific method for determining the methylation status of virtually any CpG-rich region. In addition to detecting aberrant CpG island methylation of tumor suppressor genes, MSP will be useful for monitoring CpG islands important in other biological processes. For example, MSP should facilitate monitoring patterns of methylation in imprinted genes at key stages of embryogenesis. Assays used to define clonality of cell populations, as assessed by detecting methylation patterns of X chromosome-inactivated genes in female cells, should be readily adaptable to the MSP approach. Finally, MSP should prove extraordinarily valuable clinically for the detection of methylation patterns in small DNA samples associated with disease states such as the fragile X syndrome, altered gene imprint states, and cancer.

We would like to thank Dr. Paula Vertino for helpful discussion and Dr. Ed Gabrielson for primary tumor DNA. S.M. is the recipient of an award from the Academy of Finland. This work was supported by NIH Grants 5P5-CA58184-03S1 and 5R01 CA43318-10.

1. Holliday, R. & Grigg, G. W. (1993) *Mutat. Res.* **285,** 61–67.
2. Bird, A. (1992) *Cell* **70,** 5–8.
3. Bird, A. P. (1986) *Nature (London)* **321,** 209–213.
4. Li, E., Beard, C. & Jaenisch, R. (1993) *Nature (London)* **366,** 362–365.
5. Tremblay, K. D., Saam, J. R., Ingram, R. S., Tilghman, S. M. & Bartolomei, M. S. (1995) *Nat. Genet.* **9,** 407–413.
6. Pfeifer, G. P., Steigerwald, S. D., Mueller, P. R., Wold, B. & Riggs, A. D. (1989) *Science* **246,** 810–813.
7. Riggs, A. D. & Pfeifer, G. P. (1992) *Trends Genet.* **8,** 169–174.
8. Antequera, F., Boyes, J. & Bird, A. (1990) *Cell* **62,** 503–514.
9. Herman, J. G., Latif, F., Weng, Y., Lerman, M. I., Zbar, B., Liu, S., Samid, D., Duan, D. S., Gnarra, J. R., Linehan, W. M. & Baylin, S. B. (1994) *Proc. Natl. Acad. Sci. USA* **91,** 9700–9704.
10. Merlo, A., Herman, J. G., Mao, L., Lee, D. J., Gabrielson, E., Burger, P. C., Baylin, S. B. & Sidransky, D. (1995) *Nat. Med.* **1,** 686–692.
11. Herman, J. G., Jen, J., Merlo, A. & Baylin, S. B. (1996) *Cancer Res.* **56,** 722–727.
12. Graff, J. R., Herman, J. G., Lapidus, R. G., Chopra, H., Xu, R., Jarrard, D. F., Isaacs, WB, Pitha, P. M., Davidson, N. E. & Baylin, S. B. (1995) *Cancer Res.* **55,** 5195–5199.
13. Issa, J. P., Ottaviano, Y. L., Celano, P., Hamilton, S. R., Davidson, N. E. & Baylin, S. B. (1994) *Nat. Genet.* **7,** 536–540.
14. Singer-Sam, J., Grant, M., LeBon, J. M., Okuyama, K., Chapman, V., Monk, M. & Riggs, A. D. (1990) *Mol. Cell. Biol.* **10,** 4987–4989.
15. Razin, A. & Cedar, H. (1991) *Microbiol. Rev.* **55,** 451–458.
16. Stoger, R., Kubicka, P., Liu, C. G., Kafri, T., Razin, A., Cedar, H. & Barlow, D. P. (1993) *Cell* **73,** 61–71.
17. Frommer, M., McDonald, L. E., Millar, D. S., Collis, C. M., Watt, F., Grigg, G. W., Molloy, P. L. & Paul, C. L. (1992) *Proc. Natl. Acad. Sci. USA* **89,** 1827–1831.
18. Wang, R. Y.-H., Gehrke, C. W. & Ehrlich, M. (1980) *Nucleic Acids Res.* **8,** 4777–4790.
19. Myöhänen, S., Wahlfors, J. & Janne, J. (1994) *DNA Sequence* **5,** 1–8.
20. Hara, E., Smith, R., Parry, D., Tahara, H., Steven, S. & Peters, G. (1996) *Mol. Cell. Biol.* **16,** 859–867.
21. Hussussian, C. J., Struewing, J. P., Goldstein, A. M., Higgins, P. A., Ally, D. S., Sheahan, M. D., Clark, W. H., Jr., Tucker, M. A. & Dracopoli, N. C. (1994) *Nat. Genet.* **8,** 15–21.
22. Jen, J., Harper, J. W., Bigner, S. H., Bigner, D. D., Papadopoulos, N., Markowitz, S., Willson, J. K., Kinzler, K. W. & Vogelstein, B. (1994) *Cancer Res.* **54,** 6353–6358.
23. Kuzmin, I., Duh, F. M., Latif, F., Geil, L., Zbar, B. & Lerman, M. I. (1995) *Oncogene* **10,** 2185–2194.
24. Bussemakers, M. J., Giroldi, L. A., van Bokhoven, A. & Schalken, J. A. (1994) *Biochem. Biophys. Res. Commun.* **203,** 1284–1290.
25. Herman, J. G., Merlo, A., Mao, L., Lapidus, R. G., Issa, J. P. J., Davidson, N. E., Sidransky, D. & Baylin, S. B. (1995) *Cancer Res.* **55,** 4525–4530.
26. Gonzalez-Zulueta, M., Bender, C. M., Yang, A. S., Nguyen, T., Beart, R. W., Van Tornout, J. M. & Jones, P. A. (1995) *Cancer Res.* **55,** 4531–4535.
27. Otterson, G. A., Khleif, S. N., Chen, W., Coxon, A. B. & Kaye, F. J. (1995) *Oncogene* **11,** 1211–1216.
28. Park, J. G. & Chapman, V. M. (1994) *Mol. Cell. Biol.* **14,** 7975–7983.
29. Reeben, M., Myöhänen, S., Saarma, M. & Prydz, H. (1995) *Gene* **157,** 325–329.
30. Gnarra, J. R., Tory, K., Weng, Y., Schmidt, L., Wei, M. H., *et al.* (1994) *Nat. Genet.* **7,** 85–90.
31. Yoshiura, K., Kanai, Y., Ochiai, A., Shimoyama, Y., Sugimura, T. & Hirohashi, S. (1995) *Proc. Natl. Acad. Sci. USA* **92,** 7416–7419.
32. Clark, S. J., Harrison, J., Paul, C. L. & Frommer, M. (1994) *Nucleic Acids Res.* **22,** 2990–2997.